OPTIMIZING AIRFLOW REVERSALS FOR KILN DRYING OF SOFTWOOD TIMBER BY APPLYING MATHEMATICAL MODELS*

Shusheng Pang[1]

ABSTRACT

After experimental validation of a kiln-wide drying model, a single board drying model and a stress model for kiln drying of softwood timber, these models are integrated and used to investigate benefits of airflow reversals in smoothing moisture content distribution and in reducing drying stresses for commercial kiln drying. In the current study, a high temperature drying schedule (DB/WB of 120/70°C and air velocity of 5 m/s) was simulated and 5 strategies for airflow reversal were evaluated. These strategies are: airflow reversal every hour; airflow reversal every 2 hours; airflow reversal every 3 hours and airflow reversal after 2 and 10 hours of drying. The results are compared to 'Control' in which airflow is unidirectional (no reversal). It has been found that, for the moisture content distribution, the first reversal is critical and frequencies of subsequent flow reversals can be varied depending on the drying temperature used. However, more frequent airflow reversal has benefits in reducing drying stresses. These findings are consistent with observations in commercial kiln drying of softwood lumber.

Key words: drying quality, drying schedules, moisture content, residual drying stress

INTRODUCTION

In commercial kiln drying of softwood timber, there are two major drying defects; the first one is the excessive moisture content variation in the dried timber, and the second one is the residual drying stresses and the board distortion after drying. These defects cause significant losses for foresters and wood processors due to rejection or downgrade of the wood products.

Drying conditions (air temperature, humidity and air velocity) and the changes of these conditions within a timber stack can affect the drying rate and the moisture content distribution. Fast drying is achieved by using high temperatures, high air velocities and low air humidity, but fast drying normally induces severe drying defects. One principal target for the wood drying research is to develop schedules which can achieve maximum drying rate but minimize the drying defects. After a drying schedule is chosen, air condition changes within a stack also affect drying. In the airflow direction, air temperature decreases and humidity increases, therefore, the boards in the front rows at the air inlet edge dry rapidly whereas those towards the airflow outlet edge of the stack dry more slowly (Keey and Pang, 1994).

In order to reduce the moisture content variation, the airflow is reversed periodically in commercial kiln drying of the softwood timber. Previous studies (Pang, *et al.*, 1994; Pang and Haslett, 1995) have examined different strategies for using the airflow reversals. These early studies only considered the benefits to reduce moisture content variation and concluded that two or three reversal at critical drying times may be sufficient. However, recent studies have found that the airflow has further benefits in reducing drying stress. This is particularly critical when the timber is dried using high temperatures (HT) or ultra high temperatures (UHT).

During drying, stresses develop due to moisture-content gradient and the nonuniform shrinkage properties of wood. If the residual drying stresses are not effectively relieved before the dried timber enters the subsequent process operation (remanufacturing, for example), the wood will move in a different way after re-cutting. Wood shows rheological behavior (mechano-sorptive strain and creep), which means that moisture content changes and elapsed time under stress can be used to relieve the drying stresses. The rheological properties are useful for developing strategies for reducing the stresses during and after drying.

The stress development is a complex process and the stress pattern is complicated (Pang, 2001). Therefore, it is difficult to directly measure the stress distribution in wood during drying. Mathematical modeling provides an alternative tool to examine the effect of changing wood properties or changing drying schedules on stress development during drying (Chen *et al.*, 1997; Pang, 2000).

The objective of the current study is to employ the developed mathematical models to investigate the effects of airflow reversals on smoothing moisture content distribution and reducing drying stresses. From the investigation, optimized strategies for the flow reversal are recommended. The models used in this study include a kiln wide drying model, a single drying model and a stress model for kiln drying of softwood timber.

DEVELOPMENT AND VALIDATION OF A KILN WIDE DRYING MODEL

External Heat and Mass Transfer Coefficients

To describe the drying processes of individual boards within a kiln stack it is necessary to define the boundary conditions between the wood surface and the main airstream. The heat flux (q) and the moisture mass-transfer rate (Nv) at the wood surface are defined by:

$$q = h \cdot (T_G - T_{surf}) \tag{1}$$

$$N_v = \varphi K_o \cdot \left(Y_{surf} - Y_G \right) = \beta \cdot \left(p_G^v - p_s^v \right) \tag{2}$$

in which T_{surf}, Y_{surf} and p_s^v are, respectively, the wood temperature, the air humidity and the vapour partial pressure at the wood surface and, T_G, Y_G and p_G^v are the corresponding parameters in the air stream. The heat-transfer coefficient is represented by h. The mass-transfer coefficient is β when vapour partial pressure difference is taken as driving force and is K_o when humidity difference is taken as the driving force with φ being the humidity factor. The mass-transfer coefficient related to humidity difference is a function of distance along the airflow direction from the inlet side (Kho *et al.*, 1989). The heat-transfer coefficient is correlated to the mass-transfer coefficient, as shown by Pang (1996a), and can be calculated from it. The humidity coefficient factor φ has been found to vary from 0.70 to 0.76, depending on the drying schedules and board thickness (Pang, 1994). An average value of 0.73 will be used in the following analysis.

Moisture and Heat Balance Equations

In order to describe the stack-wide drying process, constitutive equations have been developed based on heat and mass transfer, and mass and heat balance relationships. After modification of the original model, the kiln-wide model has now been extended to cover a wider range of conditions (high and low temperature drying, adsorption) and to consider variable properties of the timber.

For the moisture mass transfer and balance, the moisture loss from wood equals the moisture gain by the hot air, and the moisture-transfer rate from the board is described by mass-transfer coefficient multiplied by driving force (humidity difference, for example). These considerations yield:

$$-\frac{\partial}{\partial \tau}\left[X \cdot \rho_s \cdot (1 - \varepsilon)\right] = G \cdot \frac{\partial Y}{\partial z} = \begin{cases} -\varphi K_o \cdot a \cdot \left(Y_{surf} - Y_G\right) & \textbf{(condensation)} \\ \varphi K_o \cdot a \cdot f \cdot \left(Y_s - Y_G\right) & \textbf{(evaporation)} \end{cases} \tag{3}$$

Where X is the wood moisture content, ρs is the wood basic density, ε is the void fraction in the timber stack, a is the exposed area per unit volume of the stack and G is the dry air mass flow rate. In order to solve the above equations, the relative drying rate (f) needs to be defined which is a function of normalized moisture content (Keey and Pang, 1994; Pang, 1996b).

For the heat transfer and balance, the energy loss from the hot air equals the heat gain by the moist wood. The convective heat transfer is described by the product of heat-transfer coefficient and the temperature difference between the hot air and the wood surface. The resultant relationships are as follows:

$$\frac{\partial T_{wood}}{\partial \tau} = \frac{(1 + \alpha_R - \alpha_{LS})}{\rho_s \cdot (1 - \varepsilon) \cdot C_{Pwood}} \cdot \left[h \cdot a \cdot (T_G - T_{wood}) - G \cdot \Delta H_{wv} \cdot \frac{\partial Y_G}{\partial z} \right] \quad (4)$$

$$\frac{\partial T_G}{\partial z} = \frac{\left(h \cdot a + G \cdot C_{Pv} \dfrac{\partial Y_G}{\partial z} \right) \cdot (T_G - T_{wood})}{G \cdot (C_{Pa} + Y_G \cdot C_{Pv})} \quad (5)$$

In the above equations, T_{wood} is the wood temperature, α_R and α_{LS} are coefficients to reflect effects of heat radiation and heat loss, C_{Pwood} is the specific heat of wood, and ΔH_{wv} is the latent heat of water evaporation. Equations (1) to (5) have been solved to determine the overall average moisture content of the stack, moisture contents of individual boards, changes of air temperature and air humidity, and wood temperature along the airflow direction at different drying time.

Model Validation

Drying experiments were performed both in a tunnel dryer and in a pilot-scale commercial kiln to dry *Pinus radiata* sapwood boards. In the tests, each layer was composed of 23 sample boards, for which the density and green moisture content were determined before drying. The board cross section dimensions were 100*40 mm and the sticker thickness was 18 mm. The boards for the tunnel drying were 600 mm long with both ends being coated to minimize end drying, and the board length in the pilot-scale kiln drying was 2.3 m.

In the tunnel drying, 4 layers of the *Pinus radiata* sapwood boards were dried using drying schedules of 120/70°C and 140/90°C (dry-bulb/wet-bulb temperatures), respectively, with an air flow of 5 m/s. The flow directions were reversed every 3 hours for drying at 120/70°C and every 1.5 hours for drying at 140/90°C. During drying, the samples in the two middle layers were weighed at pre-set drying times, then moisture contents of individual boards were calculated from the recorded weights and the oven-dry weights.

For the tests in the pilot-scale kiln, six layers of green sapwood boards were used. Two layers of carefully selected and vertically matched boards were placed in the mid-height of the stack for the measurements. The drying schedule was 90/60°C with a unidirectional air velocity of 5 m/s. In the drying, the sample boards were removed after 7, 15.5, 27.5 and 39.5 hours of drying to determine the moisture contents of individual boards. The air temperatures at 5 evenly spaced points through the stack width were monitored every 20 minutes.

The experimental data from the tunnel drying tests are plotted in Figure 1 which shows the change in overall average moisture content. In the figure, the model predicted drying-rate curves are also presented for comparison with the experimental results. The experimental data and the

simulation results for the pilot-scale kiln drying are shown in Figures 2 for the moisture contents of individual boards.
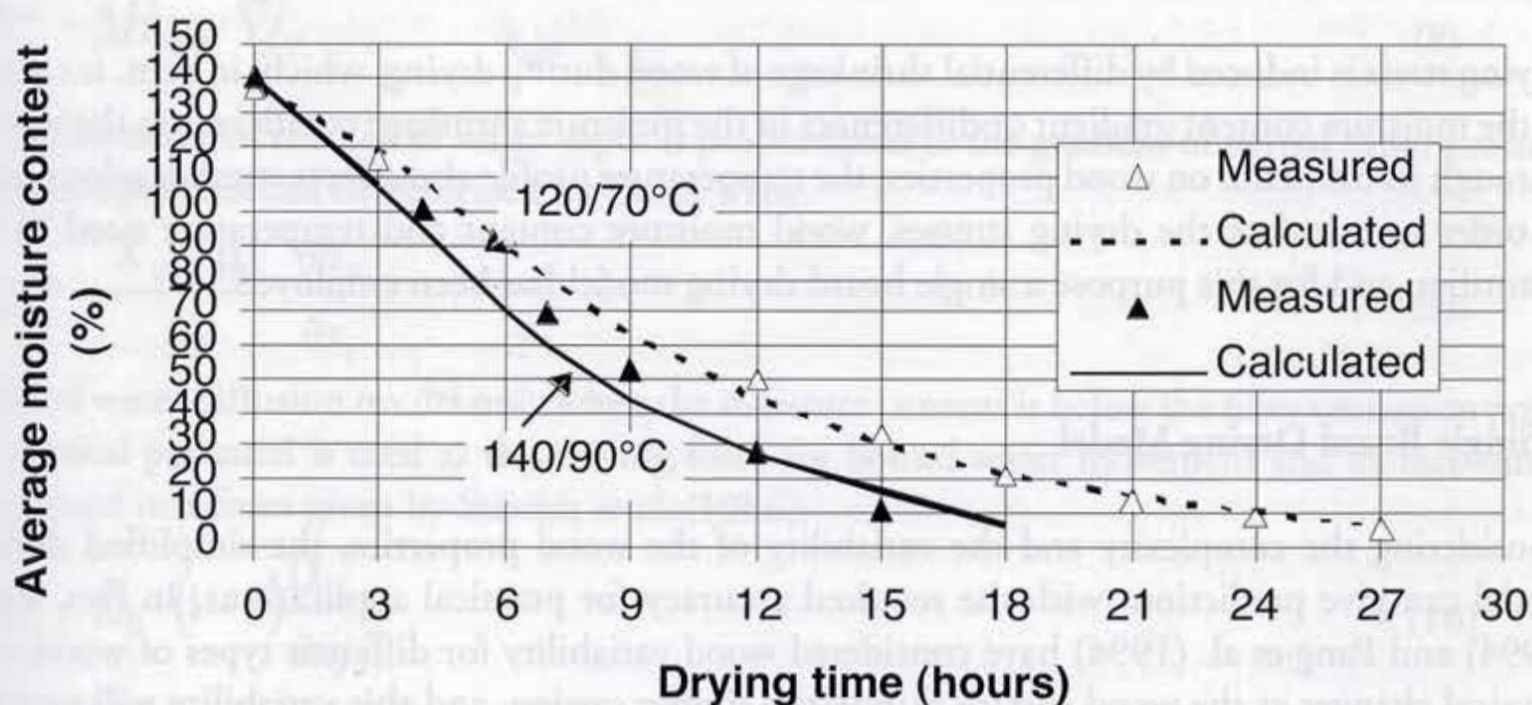

Figure 1: Measured and predicted average moisture contents over the test layer of Pinus radiata sapwood boards in a tunnel dryer.
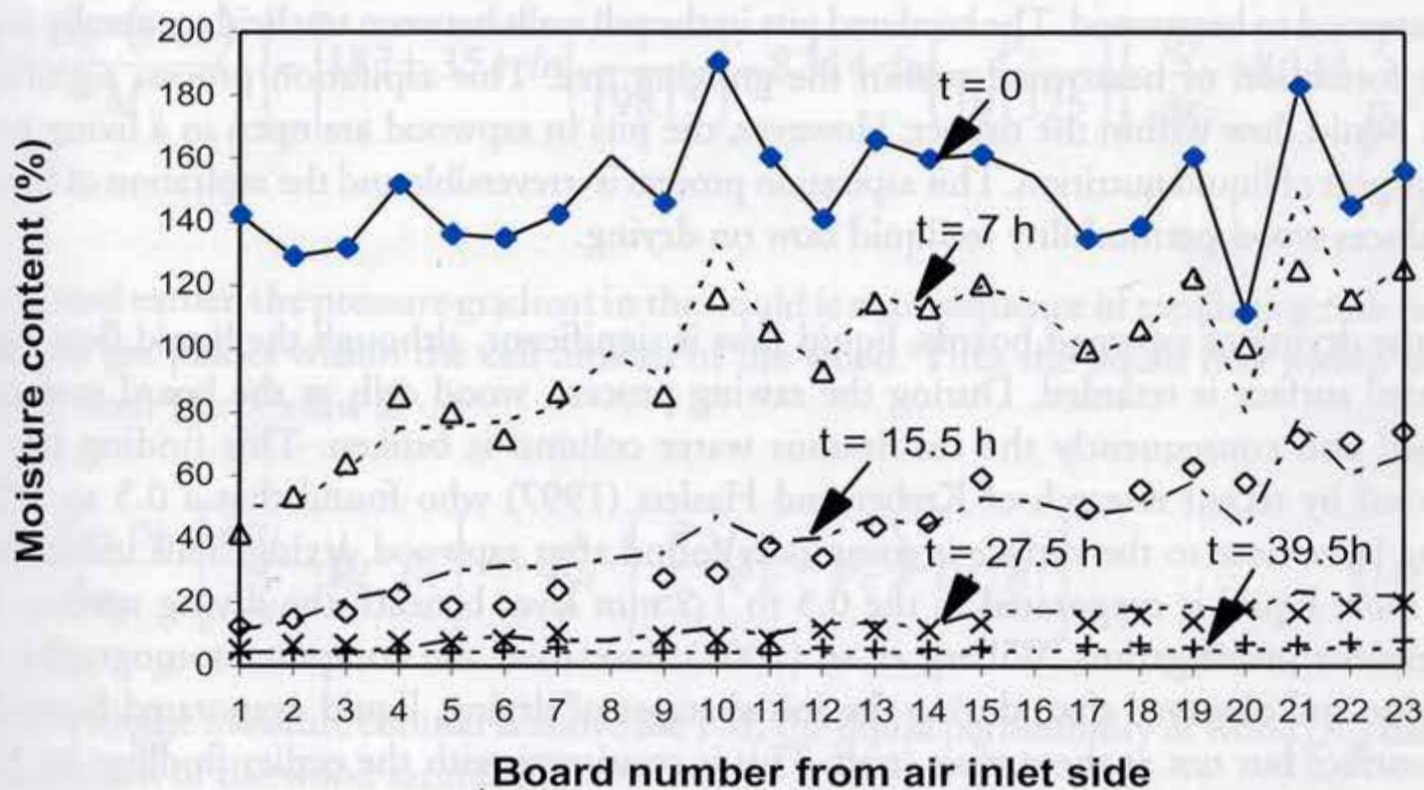

Figure 2. Moisture-contents of individual boards during drying in a pilot kiln: simulation results (lines) and comparison with experimental data (points).

The comparison of the simulated and experimental results shows that the predicted moisture contents for both the pilot-scale kiln drying and the tunnel drying are in close agreement with the measured data. The maximum discrepancy of 7% MC was observed in approximate half time of the tunnel drying at dry-bulb/wet-bulb temperatures of 140/90°C. For other two runs, the maximum discrepancy was less than 5% MC. In the above drying tests, the drying time included the time for measuring the sample weights during which the operation was stopped and the kiln door was open. Each measurement of all the sample boards took about 40 minutes. The control software recorded the kiln conditions both when the kiln was running and when the kiln was stopped, and these recorded conditions were used in the model simulation.

DEVELOPMENT AND VALIDATION OF A SINGLE BOARD DRYING MODEL AND A 1-D STRESS MODEL

Drying stress is induced by differential shrinkage of wood during drying, which, in turn, is caused by the moisture content gradient or differences in the moisture shrinkage coefficient in the wood. Through its influence on wood properties, the temperature profile also affects stress development. In order to calculate the drying stresses, wood moisture content and temperature need to be quantifies, and for this purpose a single board drying model has been employed.

A Single Board Drying Model

Considering the complexity and the variability of the wood properties, the simplified drying model can give predictions with the required accuracy for practical applications. In fact, Pang (1994) and Pang et al. (1994) have considered wood variability for different types of wood and physical changes at the wood surface during the timber sawing, and this variability will now be described.

From wood anatomy, it is known that the properties of softwood timber vary substantially from sapwood to heartwood. The bordered pits in the cell walls between tracheids generally aspirate on the formation of heartwood within the growing tree. This aspiration process significantly retards liquid flow within the timber. However, the pits in sapwood are open in a living tree for the transport of liquid nutrition. This aspiration process is irreversible and the aspiration of bordered pits reduces wood permeability to liquid flow on drying.

In the drying of sapwood boards, liquid flow is significant, although the liquid flow right to the board surface is retarded. During the sawing process, wood cells at the board surfaces are damaged and consequently the continuous water column is broken. This finding has been confirmed by recent research of Kreber and Haslett (1997) who found that a 0.5 to 1.5 mm staining layer close to the surface is commonly found after sapwood drying. This indicates that much more liquid is evaporated in the 0.5 to 1.5 mm layer beneath the drying surface. In an independent investigation, Wiberg et al. (2001) have used the computer tomography (CT) technique and observed that, during the initial stages of drying, liquid evaporated beneath the wood surface but not at the surface itself. This is consistent with the earlier findings by Kreber and Haslett (1997) and the considerations in the drying model by Pang (1994) and Pang et al. (1994).

In the simplified transport-based drying model by Pang (1994) and Pang et al. (1994), the heat and moisture mass conservation equations have the following form:

$$\frac{\partial}{\partial \tau}\left[C_P \cdot \rho_s \cdot T\right] = \nabla\left[\lambda \cdot \nabla T\right] + \Phi \tag{6}$$

$$-\rho_s \frac{\partial X}{\partial \tau} = \nabla\left(j_l + j_v + j_b\right) \tag{7}$$

In which the source term involving the latent heat of vaporisation of water is defined as:

$$\Phi = -\Delta H_{wv} \cdot \nabla j_v \tag{8}$$

It is assumed that the flux of water vapor is proportional to the gradient of partial vapor pressure, so the vapor flux can be expressed by Darcy's law:

$$j_{vi} = -\frac{K_{vi} \cdot \rho_v}{\mu_v} \cdot \frac{\partial p_v}{\partial x_i} \tag{9}$$

Bound water diffusion occurs only when the moisture content is below the fiber saturation point. Chemical potential is used as the driving force for bound water movement and its flux can be expressed in a form given by Stanish *et al.* (1986):

$$j_{bi} = -D_b \cdot (1-\varepsilon) \frac{D_{\mu b}}{\partial x_i} \tag{10}$$

From local thermodynamic equilibrium and considering that the chemical potential of bound water is the same as that for the vapor, a work form equation was derived as follows (Stanish, 1986):

$$j_{bi} = -\frac{D_b \cdot (1-\varepsilon)}{M_v} \cdot \left\{ -\left[187 + 35.1 \cdot ln\left(\frac{T}{198.15}\right) - 8.314 \cdot ln\left(\frac{p_v}{101325}\right) \right] \cdot \frac{\partial T}{\partial x_i} + 8.314 \frac{T}{p_v} \cdot \frac{\partial p_v}{\partial x_i} \right\} \tag{11}$$

As explained earlier, the pressure gradient in the liquid is a consequence of capillary action between liquid and gas phases within the cell lumens of the wood. Thus the liquid flux within wood is obtained from Darcy's law as

$$j_{li} = -\frac{K_{li} \, \rho_l}{\mu_l} \cdot \left[\frac{\partial p_l}{\partial x_i} - \rho_l \cdot g_i \right] = -E_{li} \cdot \left[\frac{\partial}{\partial x_i} (P_g - p_c) - \rho_l \cdot g_i \right] \tag{12}$$

In wood with the moisture content is above the FSP, the liquid permeability of wood (K_{li}) decreases with reduction of the wood saturation.

For softwoods, Spolek and Plumb (1981) assumed that the capillary pressure is a simple algebraic function of saturation. If the moisture content at FSP is X_{FSP} and the full saturation moisture content (or maximum moisture content) is X_{max}, then the relationship between liquid water flux and local moisture content becomes:

$$j_{li} = -\frac{7564 \cdot E_{li} \cdot (X_{max} - X_{FSP})^{0.61}}{(X - X_{FSP})^{1.61}} \cdot \frac{\partial X}{\partial x_i} \tag{13}$$

Equations from (6) to (13) can numerically be solved to calculate the fluxes of bound water (j_{bi}), water vapor (j_{vi}) and liquid water in sapwood (j_{li}). Then temperature (T) and moisture content (X) can be predicted from Equations (6) and (7). However, in solving the model, initial and boundary conditions are needed as given in Equations (1) and (2).

The model has been validated extensively by comparing the model predicted and experimentally measured average moisture content, moisture content gradient and wood temperature profiles. The details of the model validation can be found in Pang (1994) and Pang and Haslett (1995).

A 1-D Stress Model

In development of the drying stress model, the total strain (ε) is considered to be comprised of moisture shrinkage (ε_x) when the moisture content is below the fiber saturation point, stress-induced strain (either elastic or plastic, ε_σ), mechano-sorptive strain (ε_{MS}), creep strain (ε_C) and temperature effect (ε_T). The definitions of each strain component can be found in literature (Pang, 2000; 2001; Chen *et al.*, 1997). The differential form of the strain constitution equation can be written as follows:

$$d\varepsilon = \left[\frac{\partial \varepsilon_X}{\partial t} + \frac{\partial \varepsilon_\sigma}{\partial t} + \frac{\partial \varepsilon_{MS}}{\partial t} + \frac{\partial \varepsilon_C}{\partial t} + \frac{\partial \varepsilon_T}{\partial t} \right] \cdot dt \tag{14}$$

Normally, wood shrinks/swells most in tangential direction and least in the longitudinal direction. For normal wood of *Pinus radiata*, the moisture shrinkage coefficient (β) from green to oven dry is 3.4% in radial direction, 7.0% in tangential direction and 0.25% in longitudinal direction.

Where there is any restraint between successive layers of wood, the free movement of the layers is restricted to satisfy material continuity requirements (unless the material is fractured), thus the successive layers can develop different stresses. For wood, the relationship between stress and strain is also a function of moisture content, temperature, and stress level and stress history.

Mechano-sorptive strain is an important strain component of wood with drying, and occurs as a consequence of moisture content change when the wood is stressed. This behavior was derived from the observation that wood would have prolonged shrinkage or swelling when under conditions of constant load and changing moisture content (either gaining or losing moisture). During drying, this type of behavior is beneficial because it can relieve the internal constraint between layers of wood.

The creep strain reflects the deformation increment of a stressed material which increases with elapsed time. The creep process for normal material can be divided into three regions: an initial accelerating region, a constant rate region and a final rupture region which continues until the material fails. For wood, most of the reported data are for the constant rate region and for a stress level in the elastic range (Ranta-Maunus, 1993).

The above strain component equations can be used to calculate stress distribution, however, in doing so, requirements for material continuity and force balance over the cross section of a board must be satisfied.

The direct validation of the stress modelling is more complicated as the stress cannot be measured using traditional techniques. In most cases, slicing techniques are used to provide indirect quantification for the stresses which are proportional to the deformation when the stresses are relieved. The stress model has been solved to calculate stress distribution and Figure 3 shows the

stress development and relief for drying of radiate pine board at 140/90°C.

Experimental was performed to dry radiata pine sapwood boards in the tunnel dryer at dry-bulb/wet-bulb temperatures of 140/90°C (with 0.5 hour pre-heating) followed by cooling and steam conditioning at 100°C and 100% rh. During drying the circulation velocity was 7.5 m/s and this was reduced to 1.5 m/s in the cooling and the final steam conditioning. In the experiment, board average moisture content, moisture content gradient, temperature profile and stress distribution in wood were measured. The predicted stress pattern is consistent and in close agreement with the experimental results (Pang, 2000).

In drying, wood average moisture content, MC gradient and stress-induced strains in sliced layers (about 4mm in thickness) were measured and used for comparison with model predictions. The stress model was used to simulate stress development and relief for the drying conducted. The integrated model can predict the wood temperature profile, moisture content gradient, strain components, total shrinkage and stress distribution. The predicted wood temperature, moisture content gradient and drying rate curve were in close agreement with the measured data and the stress predictions were also consistent with the experimental results. The proposed stress model can reflect the actual process of stress development and relief, and thus can be applied to evaluate drying strategies in order to reduce drying stresses.

EFFECTS OF AIRFLOW REVERSALS ON RESIDUAL DRYING STRESSES

Reducing Moisture Content Variation

Along the airflow direction across the stack, the air temperature decreases and the humidity increases during drying. Therefore, reversing the airflow direction has the effect of enhancing the drying of the wetter zone and retarding the drying of the drier zone of the stack. In this way, the drying difference between the two sides of the stack can be smoothed out to a certain extent (Pang, 1994; Pang *et al.*, 1994).

In this study, a typical high temperature schedule of 120/70°C with an air velocity of 5m/s is employed and different airflow reversal strategies are evaluated. The reversing strategies which can be applied in commercial kiln operation are as follows:

- Strategy A: the airflow is reversed every hour;
- Strategy B: the airflow is reversed every 2 hours;
- Strategy C: the airflow is reversed every 3 hours;
- Strategy D: the airflow is first reversed after 2 hours and again after 10 hours (two reversals).

Strategy B and Strategy C are used in commercial kiln drying in New Zealand. Strategy A is proposed to investigate the influence of more frequent reversal whereas Strategy D is proposed to investigate the effects of only two reversals. All of these strategies are compared with 'Control' in which the airflow is maintained unidirectional (no reversal). The simulated charge consisted of flatsawn, *Pinus radiata* sapwood boards of 100x40 mm. The wood basic density is 420 kg/m³ and green moisture content is 155% which are typical values for the wood considered.

To illustrate the improvement in distribution of moisture contents across the kiln stack, the differences in moisture content through the stack with drying time from each reversal strategy are shown in Figure 4. The drying-rate curves for different strategies are similar for all of the reversal strategies and the total drying time to 10% final moisture content is from 17.5 to 17.8 hours with the control and 1 hourly reversal strategy having slightly longer drying time (17.8 hours).

The moisture content variation is described by maximum standard deviation during drying and the standard deviation at the final moisture content. From the comparison, it has been observed that:

- The first reversal is critical for reducing the peak value of the maximum differences in moisture content through a kiln-wide stack. Without airflow reversals, this peak value is 27.9% and occurs between 6.5 and 7 hours of drying. Therefore, strategies with the first reversal of 6.5 hours or earlier reduce this peak value of moisture content difference.
- The maximum moisture content variation for Strategy A is 9.6% after 5 hours of drying, and those for Strategies B and C are 12.7 and 17.4%, respectively, after 6 hours and 3 hours of drying. Interestingly, with only two reversal (after 2 and 10 hours of drying), Strategy D can also reduce the peak mc variation to 14%.
- At the final moisture content of 10%, all of the reversal strategies can achieve a low standard deviation of 2.3%, whereas without airflow reversal the variation is 7.3%.
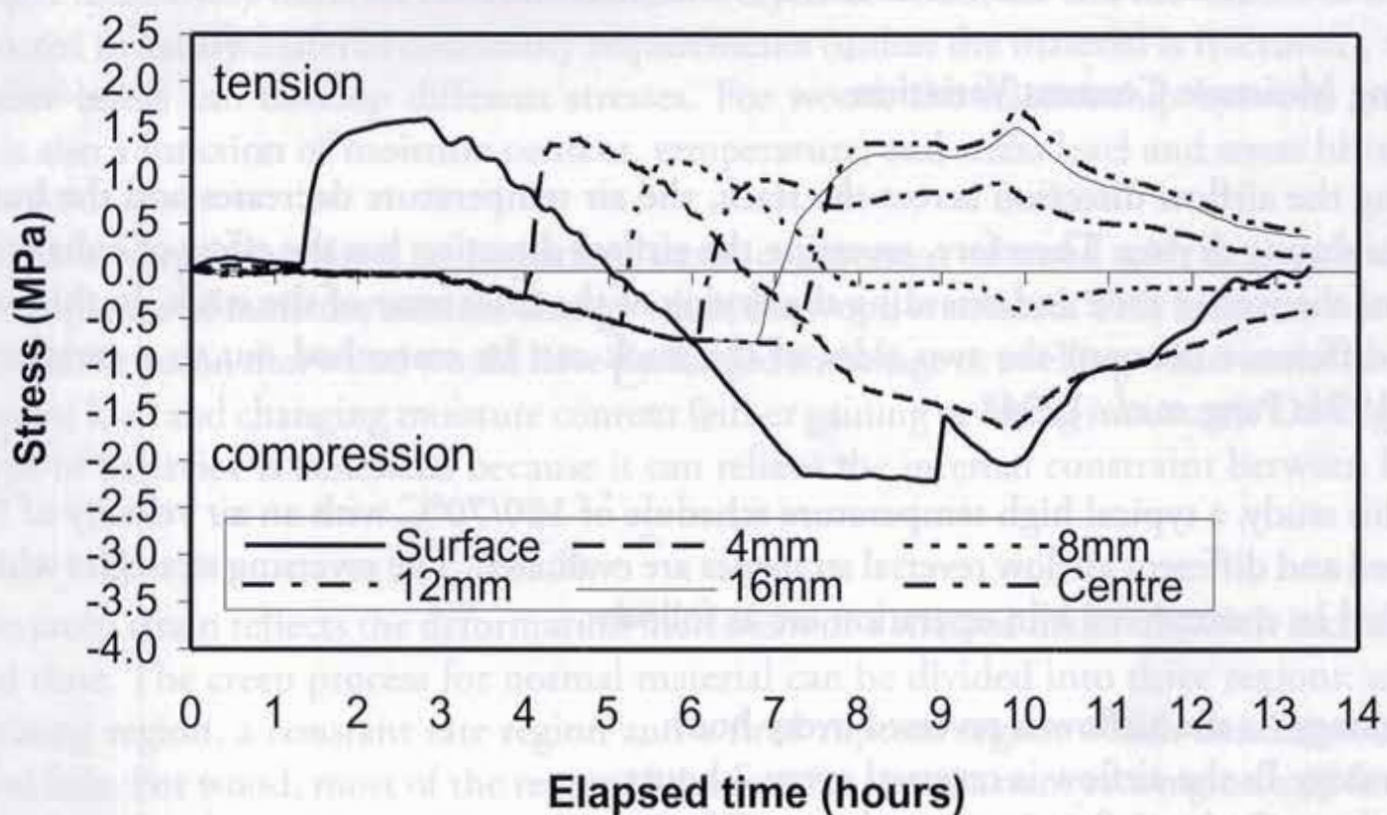

Figure 3. Predicted stress profile in a 100x40 mm sapwood board during drying (140/90°C, 7.5 m/s), cooling and steaming.
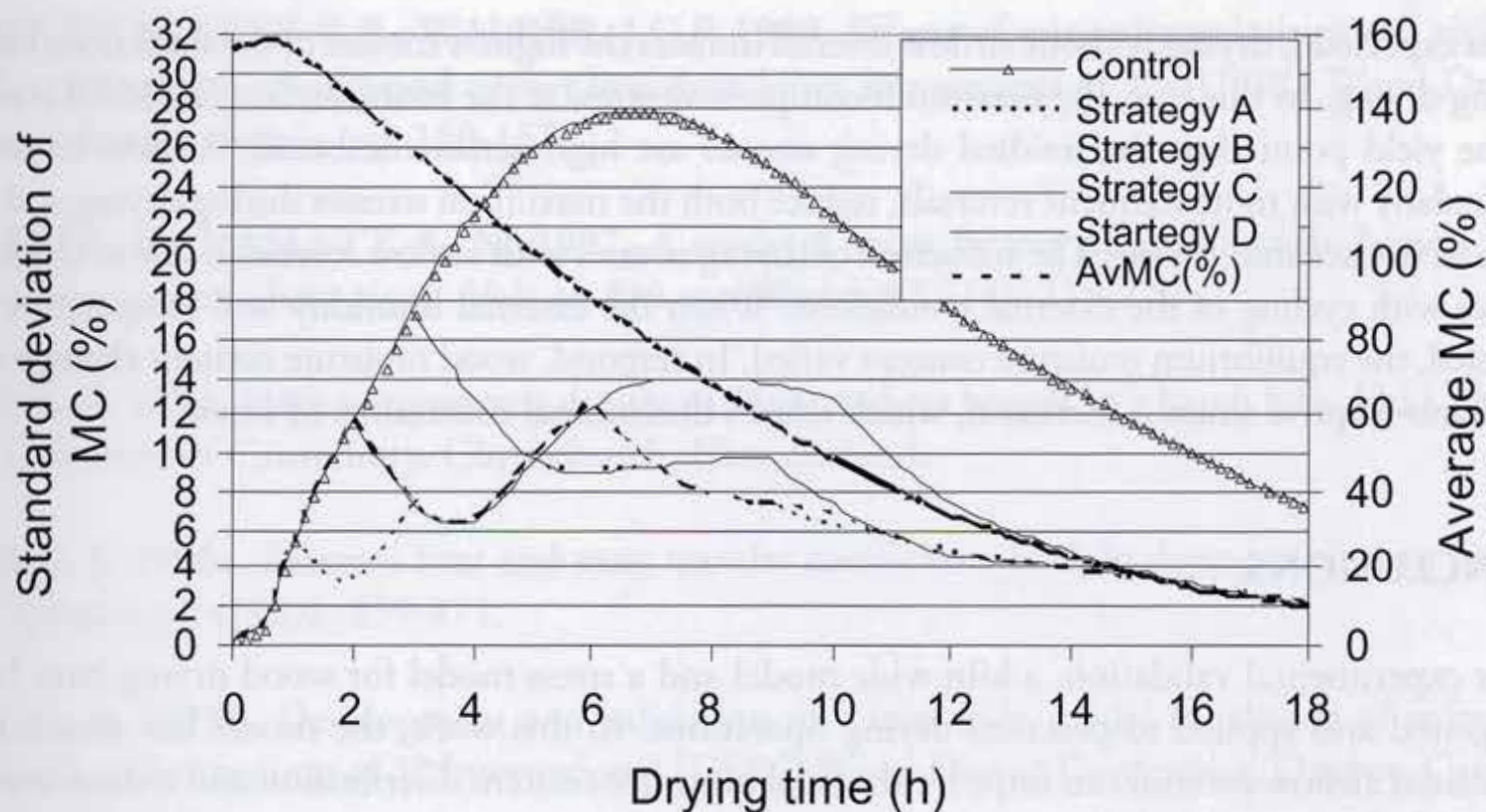
Figure 4. Comparison of moisture content variations within a 2.4 wide kiln stack between different airflow reversal strategies

Reducing Drying Stresses

In order to investigate the effects of airflow reversals on the stress development during drying, both of the kiln-wide drying model and the stress model have been used. Firstly the kiln-wide drying model was run to define the drying conditions over an edge board, which represents the harshest drying conditions through the stack. Then the stress model was used to calculate the stresses in wood at different depths from the flat drying surface. The simulated charge and the airflow reversal strategies are the same as in the moisture content simulation described in the previous section.

The simulation results are summarized in Table 1 which shows the maximum drying stresses during drying and the residual stresses after drying to an overall average moisture content of 10%. The stress status (tensile or compressive) and locations are also indicated.

Table 1. Maximum stress during drying and residual stress after drying (Dry-bulb/wet-bulb temperatures of 120/70°C, air velocity of 5 m/s, 100x40 mm *Pinus radiata* sapwood board)

Airflow Strategies	Maximum stresses (Depths, Drying time)	Stresses (Depths) After drying
Control	+1.5 MPa (2 mm, 5.8h)	+1.1 MPa (centre)
	-2.8 MPa (surface, 15.4h)	-2.8 MPa (surface)
A	+1.4 MPa (2mm, 8.64h)	+1.0 MPa (12mm)
	-1.4 MPa (surface, 17.5h)	-1.4 MPa (surface)
B	+1.5 MPa (2mm, 8.81h)	+1.0 MPa (12mm)
	-1.6 MPa (surface, 17.5h)	-1.6 MPa (surface)
C	+1.5 MPa (2mm, 7.81h)	+1.0 MPa (10mm)
	-1.8 MPa (surface, 17.6h)	-1.8 MPa (surface)
D	+1.5 MPa (2mm, 11h)	+1.0Mpa (10mm)
	-1.7 MPa (surface, 17.6h)	-1.7 MPa (surface)

As expectedd, drying without airflow reversal induces the highest stresses in the stack front board during drying. In this case, the maximum compressive stress at the board surface (2.8MPa) is close to the yield point thus the residual drying stresses are high across the board. Airflow reversals, particularly with more frequent reversals, reduce both the maximum stresses during drying and the residual stresses after drying. The reduction of drying stresses with airflow reversal is due to the stress relieve with cycling of the external conditions. When the external humidity and temperature are recycled, the equilibrium moisture content varied. In respond, wood moisture content changes and mechano-sorptive strain is increased, which relaxes the internal constraints of wood.

CONCLUSIONS

After experimental validation, a kiln wide model and a stress model for wood drying have been integrated and applied to practical drying operations. In this work, the model has shown that optimized airflow reversal can improve the final moisture content distribution and reduce stresses during drying or residual stresses after drying.

All of the airflow reversal strategies examined can reduce the moisture content variation by reducing the standard deviation from 7.3% to 2.3%mc. The high maximum MC variation during drying increases the number of boards with extremely low or high moisture contents after drying. Therefore it is also beneficial to reduce the peak moisture content variation during drying. As this peak variation occurs at about one-third of the full drying time, the first airflow reversal before this time is necessary. For the purpose of reducing the peak moisture content variation, airflow reversal every 2 hours or two reversals after 2 and 10 hours can give similar results as airflow reversal every one hour.

Airflow reversals, particularly with more frequent reversals, also reduce the maximum stresses during drying and the residual stresses after drying. The most frequent flow reversal (every hour) gives the lowest maximum stress during drying and the lowest residual stress after drying. However, in considering the practical operation and idle time in switching over the fan direction, airflow reversal every 2 hours is recommended. This policy should change with drying temperature. With lower drying temperatures, the span of the reversal can be lengthened, for example, for accelerated drying temperature (ACT) which is widely applied in kiln drying of *Pinus radiata* lumber, airflow reversal every 4 hours are recommended. For higher temperature (140°C) or ultra high temperature (>160°C), airflow direction should be reversed every hour or every half hour.

REFERENCES

CHEN, G.; KEEY, R.B.; WALKER, J.C.F. 1997. The drying stress and check development on high temperature kiln seasoning of sapwood *Pinus radiata* boards. *Holz als Roh- und Werkstoff* 55 (2):59-64.

KEEY, R.B.; PANG, S. 1994. The high temperature drying of softwood boards: A kiln wide model. *Chemical Engineering Research and Design* 72(A6):741-753.

KHO, P.C.S.; KEEY, R.B.; WALKER, J.C.F. 1989. Effects of minor irregularities and airflows on drying rate of softwood timber boards in kilns. Proceedings of 2nd IUFRO Wood Drying Conference, Seattle, pp. 150-157.

KREBER, B.; HASLETT, A. N. 1997. A study of some factors promoting kiln brown stain formation in radiata pine. *Holz als Roh und Werkstoff* 55 (4): 215-220

PANG, S. 1994. High temperature drying of *Pinus radiata* boards in a batch kiln. PhD Thesis, University of Canterbury, Christchurch, New Zealand.

PANG, S. 1996a. External heat and mass transfer coefficients for kiln drying of timber. *Drying Technology* 14(3&4):859-871.

PANG, S. 1996b. Development and validation of a kiln-wide model for drying of softwood lumber. Proceedings of 5th International IUFRO Wood Drying Conference, Quebec, Canada, pp.103-110.

PANG, S. 2000. Modelling of stress development during drying and relief during steaming in *Pinus radiata* lumber. Drying Technology 18(8):1677 – 1696.

PANG, S. 2001. Modeling of stresses and deformation of radiata pine lumber during drying. Proceedings of 7th IUFRO Wood Drying Conference, pp.238-245.

PANG, S.; HASLETT, A.H. 1995. The application of mathematical models to the commercial high temperature drying of softwood lumber. *Drying Technology* 13(8&9): 1635-1674.

PANG, S.; KEEY, R.B.; WALKER, J.F.C. 1994. Airflow reversals in high temperature kiln drying of *Pinus radiata* boards 2: Drying of a stack of boards. *New Zealand Journal of Forestry Science* 24(1):104-119.

RANTA-MAUNUS, A. 1993. Rheological behavior of wood in directions perpendicular to the grain. *Materials and Structure* 2:362-369.

SPOLEK, G. A. ; PLUMB, O. A. 1981. Capillary Pressure in Softwood. *Wood Science and Technology* 15: 189 - 199.

STANISH, M.A. 1986. The roles of bound water chemical potential and gas phase diffusion in moisture transport through wood. *Wood Science and Technology* 19: 53-70.

STANISH, M.A.; SCHAJER, G.S.; KAYIHAN, F. 1986. A mathematical model of drying for hygroscopic porous media. *AIChE Journal* 32(8): 1301-1311.

WIBERG, P.; SEHLSTEDT, S.M.B.; MORÉN, T.J. 2001. Heat and mass transfer during sapwood drying above the fibre saturation point. *Drying Technology* 18(8): 1647-1664.

NOTATION

a	:	exposed surface per unit stack volume (m^2 m^{-3})
C_P	:	specific heat of wet wood (J kg^{-1} K^{-1})
C_{Pa}	:	specific heat of dry air (J kg^{-1} K^{-1})
C_{Pv}	:	specific heat of vapor (J kg^{-1} K^{-1})
C_{Pwood}	:	specific heat of dry wood (J kg^{-1} K^{-1})
D_b	:	bound water diffusion coefficient (kg s m^{-2})
f	:	relative drying rate
G	:	air mass flow rate (kg m^{-2} s^{-1})
h	:	heat-transfer coefficient (W m^{-2} K)
j	:	flow rate (kg m^{-2} s^{-1})
K	:	wood permeability (m^2)
M_v	:	molar weight of vapor (kg mol^{-1})
N_v	:	mass transfer rate (kg m^{-2} s^{-1})
p_c	:	capillary pressure (Pa)
P_g	:	gas pressure in wood (Pa)
p_G^v	:	vapor partial pressure in the main stream (Pa)
p_S^v	:	vapor partial pressure at wood surface (Pa)
q	:	heat transfer rate (W m^{-2})
t	:	time (s)
T_G	:	air temperature in the main stream (K)
T_{surf}	:	wood surface temperature (K)
T_{wood}	:	wood temperature (K)
X	:	moisture content (kg kg^{-1})
X_{FSP}	:	fiber saturation point (kg kg^{-1})
X_{max}	:	maximum moisture content at full saturation (kg kg^{-1})
Y_G	:	air humidity in the main stream (kg kg^{-1})
Y_s	:	air humidity at saturation (kg kg^{-1})
Y_{surf}	:	air humidity at wood surface (kg kg^{-1})
z	:	distance along the air flow direction (m)

GREEKS

α_R	:	radiation factor
α_{LS}	:	heat loss factor
β	:	mass-transfer coefficient based on vapor partial pressure (s m^{-1})
ε	:	void fraction in stack and in wood (m^3 m^{-3})
ε	:	wood strain (m m^{-1})
φK_o	:	mass-transfer coefficient based on air humidity (kg m^{-2} s^{-1})
λ	:	heat conductivity of wood (W m^{-1} K^{-1})
μ_b	:	chemical potential of bound water (J kg^{-1})
ρ	:	density (kg m^{-3})
ρ_s	:	wood basic density (kg m^{-3})
τ	:	time (s)
ΔH_{wv}	:	latent heat of vaporization (J kg^{-1})

Subscript:

i	:	space coordinate in one of the three directions
v	:	vapor
b	:	bound water
l	:	liquid water